Nanohybrids of Mg/Al layered double hydroxide and long-chain (C18) unsaturated fatty acid anions: structure and sorptive properties

Rafael Celis [a,*], M. Ángeles Adelino [a], Beatriz Gámiz [a], M. Carmen Hermosín [a], William C. Koskinen [b], Juan Cornejo [a]

[a] *Instituto de Recursos Naturales y Agrobiología de Sevilla (IRNAS), CSIC, Avenida Reina Mercedes 10, Apartado 1052, 41080 Sevilla, Spain*

[b] *USDA-ARS-University of Minnesota, 1991 Upper Buford Circle, 439 Borlaug Hall, St.Paul, MN 55108, USA*

Corresponding author:

Dr. Rafael Celis

Address: Instituto de Recursos Naturales y Agrobiología de Sevilla (IRNAS), CSIC

Avenida Reina Mercedes 10, Apartado 1052

41080 Sevilla

Spain.

Phone: +34 954624711

Fax: +34 954624002

E-mail: rcelis@irnase.csic.es

ABSTRACT

Long-chain (C18) unsaturated fatty acid anions, elaidate (ELA), oleate (OLE), linoleate (LINO), and linolenate (LINOLEN), were intercalated into Mg/Al (3:1) layered double hydroxide (LDH) and the resultant organo-LDH nanohybrid materials were characterized and subsequently evaluated as sorbents of six pesticides (clopyralid, imazethapyr, diuron, atrazine, alachlor, and terbuthylazine). The effect of the degree (18:1, 18:2, 18:3) and type (*cis*/*trans*) of unsaturation in the fatty acid alkyl chain on both the structure and sorptive properties of the LDH-unsaturated fatty acid nanohybrids were determined. All fatty acid anions were readily intercalated into the LDH, yielding structures with basal spacing values ranging between 32 Å (LDH-LINOLEN) and 40 Å (LDH-ELA). The bend imposed by the *cis* geometry of the double bonds present in OLE, LINO and LINOLEN was identified as a major factor determining the arrangement of these anions in the LDH interlayer space. Intercalation of *cis*-unsaturated fatty acid anions led to less densely packed structures and reduced the interlayer distance of the resultant nanohybrid compared to the structures resulting from intercalation of the linear, *trans*-unsaturated elaidate anion. All organo-LDHs displayed higher affinity to uncharged pesticides as compared to unmodified LDH, but double bonds in the fatty acid alkyl chain, particularly when present in *cis* configuration, reduced the affinity of the organo-LDHs to all pesticides, presumably because they led to structures with reduced hydrophobicity as compared to those resulting from the incorporation of linear organic anions.

Keywords: Adsorption; Bionanocomposites; Fatty acids; Hydrotalcite; Pesticides; Pollution

1. Introduction

Layered double hydroxides (LDHs), also known as anionic clays or hydrotalcite-like compounds, are a special group of layered materials. Their structure consists of positively charged brucite-type layers of mixed divalent (M^{II}) and trivalent (M^{III}) metal hydroxide, $[M^{II}_{1-x}M^{III}_{x}(OH)_2]^{x+}$, where the positive charge is balanced by exchangeable hydrated anions ($A_{x/n}^{n-}\cdot mH_2O$) located in the interlayer space (Cavani et al., 1991; Rives, 2001). LDHs have recently gained much attention because of their broad applications as sorbents, anionic exchangers, base catalysts, polymer additives, etc. (Cavani et al., 1991; Paek et al., 2011; Rives, 2001). In particular, the great interest in LDHs as sorbent materials is related to their anionic exchange properties, the large specific surface areas associated with their layered nanostructure, the ease with which they are synthesized, and the possibility of modifying their surfaces to increase their affinity for specific sorbates (Cornejo et al., 2008; Lagaly, 2001).

Because of their anion exchange properties, LDHs often display a high affinity for anionic contaminants. Furthermore, the calcination product of various LDHs (e.g., 500 ºC) is a mixed oxide, which has the peculiarity that it can rehydrate from water containing anions to reconstruct the original LDH layered structure (Miyata, 1980), a property known as "memory effect" (Cavani et al., 1991; Chibwe and Jones, 1989; Narita et. al., 1991). Accordingly, both LDHs and their calcined products have been proposed as sorbents to remove anionic pollutants from aqueous solutions, either by an anionic exchange mechanism or by the reconstruction mechanism or memory effect (Cardoso and Valim, 2006; Hermosín et al., 1993; Inacio et al., 2001; Sato and Okuwaki, 1991).

The anionic exchange properties of LDHs also allow the intercalation of a wide variety of organic anions in the LDH interlayer space to yield the so-called organo-LDHs (Ayala-Luis et al., 2010; Clearfield et al., 1991; Costantino et al., 2009; Meyn et al., 1990; Miyata and Kumura, 1973). Many short and long-chain alkyl carboxylates, alkyl sulfates, and alkyl sulfonates have been intercalated into LDHs, expanding the interlayer and rendering the LDH

surfaces hydrophobic (Costa et al., 2008; Meyn et al., 1990; Newman and Jones, 1998; Pavlovic et al., 1997; Xu et al., 2004). Combination at the nanometric scale of the expansive surface areas, anisotropic shape and reactive surfaces of LDHs with the functional and/or hydrophobic behavior of organic anions has been pointed out as an attractive way to develop organic-inorganic nanohybrid materials with properties that are inherent to both types of components (Paek et al., 2011). How organic anions are intercalated and packed in the interlayer is the theme of much current research (Xu and Braterman, 2010). In an environmental context, the study of organo-LDHs as sorbents for the removal or immobilization of organic pollutants is also a current research goal (Ayala-Luis et al., 2010; Bruna et al., 2012; Celis et al., 1999; Cornejo et al., 2008; Villa et al., 1999; Zhao and Nagy, 2004).

As for long-chain alkyl carboxylates, the structures resulting from the intercalation of saturated fatty acids, such as lauric, myristic, palmitic and stearic acids, into LDHs have extensively been characterized (Ayala-Luis et al., 2010; Borja and Dutta, 1992; Carlino, 1997; Costantino et al., 2005; Iyi et al., 2009; Kuehn and Pollmann, 2010); however, little is known about the structure of organo-LDHs prepared by intercalation of unsaturated fatty acids and even less about their sorptive properties (Inomata and Ogawa, 2006; Kameshima et al., 2006). Most previous studies have focused on the structural characterization of LDH-oleate nanohybrids (Donato et al., 2012; Inomata and Ogawa, 2006; Kameshima et al., 2006; Xu et al., 2004). We found only one comparative study on the intercalation of elaidate and oleate anions (Xu et al., 2004), and none on the intercalation of polyunsaturated analogues such as linoleate or linolenate.

The presence of one or more double bonds in the alkyl chain is expected to affect significantly the packing mode of the intercalated surfactant (Kanicky and Shah, 2002). In particular, for fatty acids containing *cis*-unsaturated chains, the *cis* geometry imposes a bend in the alkyl chain which can disrupt the arrangement of the organic anions in the LDH interlayers.

Thus, the structure and properties of organo-LDHs are expected to vary depending on the number, position, and configuration of the double bonds within the alkyl chain. Lagaly et al. (1977) stressed the importance of the effect of unsaturation on the structures resulting after intercalation of alkylammonium ions into smectite; however, as for LDHs, the intercalation of unsaturated anionic surfactants has scarcely been investigated (Inomata and Ogawa, 2006). *Cis*-unsaturated fats are natural compounds conventionally regarded as healthier than saturated fats. Consequently, the use of unsaturated fatty acid anions for LDH modification would reduce concern about the incorporation of the resulting materials into soil and aquatic environments for practical applications compared to the use of their saturated analogues and other anionic surfactans (Cruz-Guzmán et al., 2004).

In the present study, four long-chain (C18) unsaturated fatty acid anions (elaidate, oleate, linoleate, and linolenate) (Fig. 1) were intercalated into a Mg/Al (3:1) LDH using the reconstruction method (memory effect). The resultant organo-LDHs were characterized and subsequently evaluated as sorbents of six pesticides with different chemical structures. By using different unsaturated fatty acids with the same chain length (C18), we aimed at assessing whether the degree and type of unsaturation in the fatty acid affected the structure and sorptive properties of the resultant nanohybrids. Dodecylsulfate-intercalated LDH was also prepared, characterized, and assayed as a pesticide sorbent for comparative purposes.

2. Materials and methods

2.1. Sample preparation

The starting carbonate-Mg:Al (3:1) LDH was prepared by the conventional coprecipitation method (Reichle, 1986). An aqueous solution (100 mL) containing 0.3 mol of $Mg(NO_3)_2 \cdot 6H_2O$ and 0.1 mol of $Al(NO_3)_3 \cdot 9H_2O$ was added dropwise to an alkaline solution (500 mL) containing 1.6 mol of NaOH and 0.37 mol of Na_2CO_3. The precipitate obtained was hydrothermally treated at 80 ºC for 24 h, washed with deionized water, and then freeze-dried.

Elaidate (ELA)-, oleate (OLE)-, linoleate (LINO)-, and α-linolenate (LINOLEN)-intercalated LDH samples were prepared by the reconstruction method from calcined-LDH, i.e. the product resulting from heating the LDH sample at 500 ºC for 3 h, following a procedure similar to that described by Chibwe and Jones (1989). For the synthesis, 500 mg of calcined-LDH (containing 2.6 mmol of Al) was added to 110 mL of aqueous solutions containing 3 mmol of elaidic, oleic, linoleic, or α-linolenic acid (Sigma-Aldrich, Spain) plus 3.3 mmol of NaOH, which was added to ensure the conversion of the fatty acids to the respective sodium salts. The dissolution of the fatty acid sodium salts was favored by gentle heating at 60 ºC. The dodecylsulfate (DDS)-intercalated LDH sample was synthesized by adding 500 mg of calcined-LDH to 110 mL of an aqueous solution containing 3 mmol of sodium dodecylsulfate (Sigma-Aldrich, Spain) and 0.3 mmol of NaOH. A blank "reconstructed LDH" sample was also prepared by adding 500 mg of calcined-LDH to 110 mL of an organic acid-free aqueous solution containing 0.3 mmol of NaOH. All dispersions were shaken for 24 h at 60 ºC, and the resultant organo-LDHs and reconstructed LDH sample were washed with warm deionized water (60 ºC), filtered (0.45 μm), air-dried, and stored at room temperature in the dark until used.

2.2. Sample characterization

Sample characterization was conducted by element chemical analysis, Fourier-transform infrared spectroscopy (FT-IR), X-ray diffraction (XRD), scanning (SEM) and transmission (TEM) electron microscopy, and zeta potential measurements. Element chemical analysis of Mg and Al was conducted by inductively coupled plasma-optical emission spectroscopy (ICP-OES) using a Varian ICP 720-ES instrument after digestion of 20 mg of LDH sample with 1 mL of 37% HCl, whereas the CHNS element chemical analysis was conducted using a Perkin-Elmer, model 1106, element analyzer. The stability of the organo-LDHs in aqueous dispersion was evaluated by shaking 20 mg of organo-LDH in 10 mL of 0.01 M $CaCl_2$ for 24 h, and then

131 determining the amount of organic carbon released into the solution by the samples using a
132 Shimadzu TOC-V sch total organic carbon analyzer. Fourier-transform infrared (FTIR) spectra
133 were recorded using a Jasco FT/IR 6300 spectrometer (Jasco Europe s.r.l.) directly placing the
134 solid samples in a horizontal-trough, attenuated total reflectance (ATR) cell. Powder X-ray
135 diffraction patterns were obtained with a Bruker D8 Discover diffractometer using CuK_α
136 radiation (λ= 0.15418 nm) at a scanning speed of $2\Theta = 2^o$ min^{-1}. The structures proposed for the
137 organo-LDHs were generated from XRD data assuming a brucite-like layer thickness of 4.8 Å
138 (Cavani et al., 1991), an average Al-Al distance in the 3:1 Mg:Al hydroxide layer of ~ 6 Å,
139 resulting from considering that Mg^{2+} and Al^{3+} cations were regularly distributed in the LDH
140 layer (Zhao and Nagy, 2004), and the organic anion molecular structures generated by
141 ACD/Chemsketch software, which was also used to determine the interatomic distances in the
142 organic anions. Scanning and transmission electron micrographs were obtained using a Hitachi
143 S5200 and a Hitachi H800 electron microscope, respectively. Zeta potential measurements
144 were carried out with a Malvern Zetasizer Nano ZS Instrument using aliquots of 1.5 mg of
145 sample dispersed in 1 mL of deionized water.
146
147 *2.3. Sorption experiments*
148 The sorption of six pesticides (clopyralid, imazethapyr, diuron, atrazine, alachlor, and
149 terbuthylazine) (Fig. 2) on the LDH materials prepared in this work was studied by the batch
150 equilibration procedure using glass centrifuge tubes lined with screw caps. Aliquots of 20 mg
151 of LDH, calcined-LDH or organo-LDH sorbent samples were equilibrated by shaking for 24 h
152 at 20 ± 2 ºC with 8 ml of an aqueous solution with an initial pesticide concentration, C_{ini}, of 1
153 mg L^{-1}. After equilibration, the dispersions were centrifuged and 4 mL of the supernatant
154 solution was removed, filtered and analyzed by high performance liquid chromatography
155 (HPLC) to determine the pesticide equilibrium concentration, C_e (mg L^{-1}). The amount of

pesticide sorbed, C_s (mg kg^{-1}), was determined from the difference between the initial and equilibrium solution concentrations. Pesticide initial solutions without sorbent were also prepared and served as controls to determine possible losses of the pesticides due to processes other than sorption to the solids. Percentages of pesticide sorbed (% Sorbed) were calculated by using the following formula: %Sorbed= $[(C_{ini}-C_e)/C_{ini}] \times 100$, whereas sorption distribution coefficients, K_d (L kg^{-1}) were calculated as $K_d= C_s/C_e$. Organic carbon-normalized K_d values ($K_{d\text{-}oc}$) for the sorption of the pesticides on the organo-LDHs were calculated by dividing the sorption distribution coefficients, K_d, by the organic carbon content of the organo-LDHs. Relevant physicochemical properties of the pesticides and details on the chromatographic conditions used for their analysis by HPLC are included in Tables S1 and S2 of the Supplementary information.

3. Results and discussion

3.1. Chemical analysis

Table 1 shows the results of the element chemical analysis of LDH, calcined LDH, and the organo-LDHs prepared in this work, together with some relevant molar ratios. The empirical formula for each sample was derived from the results of the element chemical analysis, assuming a hydrotalcite-like structure (for LDH and the organo-LDHs) or a mixed oxide structure (for calcined LDH). The Mg and Al content of the samples was used to calculate the composition of the hydroxide layer, whereas the C content was used to calculate the amount of carbonate in LDH and the amount of organic anion in the organo-LDHs. The amount of water in the proposed formula (Table 1), roughly estimated by difference, was found to be in reasonable agreement with the mass loss of the samples upon drying at 150 ºC for 4 h.

For all samples, the Mg:Al ratio was close to the expected value of 3 (x~ 0.25), thus revealing the complete coprecipitation of the structural metals during the synthesis of the pristine LDH. The C to Al ratio of LDH (C/Al= 0.60) was slightly greater than the value

182 expected if all anion exchange sites in LDH were occupied by CO_3^{2-} anions (C/Al= 0.5). A
183 possible explanation for this finding is that HCO_3^- species appeared during the successive
184 washings of the sample as a result of a decrease in the pH of the solution. As for the organo-
185 LDHs, the C to Al ratio was close to the expected value of 18 for the fatty acid anions and 12
186 for DDS, which revealed that all organic anions were successfully incorporated into the LDH
187 structure during the reconstruction reaction conducted to prepare the organo-LDH samples.
188 Actually, data in Table 1 show that the C to Al ratio was slightly less than the expected one
189 (C/Al= 12) for DDS, but slightly larger than the expected one (C/Al= 18) for all fatty acids.
190 Most likely, a small fraction of the fatty acids existed in the nanohybrids in their sodium salt
191 forms (Costantino et al., 2009). It is also worthy to note that the organo-LDHs displayed a
192 considerable stability in aqueous dispersion, but the stability depended on the intercalated
193 anion. The amount of organic carbon released by the organo-LDHs when shaken for 24 h in
194 0.01 M $CaCl_2$ was < 2% for LDH-DDS, LDH-ELA, and LDH-OLE, 2.8% for LDH-LINO, and
195 13% for LDH-LINOLEN. Thus, intercalation of the polyunsaturated anions appeared to result
196 in somewhat less stable structures compared to those resulting from intercalation of the
197 saturated and mono-unsaturated anions.
198
199 *3.2. Fourier-transform infrared (FT-IR) spectroscopy*
200 The FT-IR spectra of LDH, calcined LDH, reconstructed LDH, and the organo-LDHs
201 prepared in this work are shown in Fig. 3. The FT-IR spectrum of LDH was typical of Mg:Al
202 layered double hydroxide containing carbonate as interlayer anion. It showed the characteristic
203 absorption bands of structural hydroxyl groups and adsorbed and intercalated water molecules
204 at 3500, 3000 and 1650 cm^{-1}, interlayer carbonate species at 1365 cm^{-1}, and metal-oxygen
205 lattice vibrations below 1000 cm^{-1} (Cavani et al., 1991; Costa et al., 2008; Hernández-Moreno
206 et al., 1985). The FT-IR spectrum of calcined LDH revealed an almost complete
207 dehydroxylation and decarbonation of the mineral. The small shoulders observed at about

208 3400, 1650, and 1405 cm^{-1} (Fig. 3) indicated the presence of some water molecules and
209 carbonate ions, which probably became adsorbed on the calcined powder upon its exposure to
210 air (Barriga et al., 2002; del Arco et al., 1993; Goh et al., 2009). The spectrum of the blank
211 reconstructed LDH sample resembled that of the original LDH, proving the successful
212 recovery of the LDH structure upon rehydration and carbonation of the calcined product.
213 In the FT-IR spectra of the organo-LDHs, the appearance of new bands compared to those
214 observed in the spectrum of the original LDH provided further evidence for the presence of the
215 organic anions in the samples. A detailed assignation of these bands is given in Table S3 of the
216 Supplementary information. In the FT-IR spectra of LDH-ELA, LDH-OLE, LDH-LINO and
217 LDH-LINOLEN, the C-H stretching vibrations of the alkyl chains appeared at about 2955,
218 2922, and 2852 cm^{-1}, whereas the band at 1466 cm^{-1} can be attributed to the C-H bending
219 vibration mode. Notably absent in the spectra were the shoulder at 3000 cm^{-1}, corresponding to
220 water molecules strongly associated with interlayer carbonate anions, and bands corresponding
221 to the protonated -COOH groups of the fatty acids. In contrast, we observed two bands at about
222 1544 and 1406 cm^{-1}, which can be assigned to the antisymmetric and symmetric stretching
223 vibration modes of carboxylate groups (Costa et al., 2008; Iyi et al., 2009; Xu et al., 2004).
224 These bands evidenced that the fatty acids were incorporated into the LDH structure in their
225 ionized forms. All these bands were in agreement with those previously reported by other
226 authors for LDHs intercalated with saturated carboxylic acids, but we also observed in our
227 spectra distinctive features of the unsaturations present in ELA, OLE, LINO, and LINOLEN.
228 Thus, the characteristic stretching vibration band for C-H groups adjacent to a *cis* double bond
229 was identified in the spectra of LDH-OLE, LDH-LINO, and LDH-LINOLEN near 3010 cm^{-1},
230 whereas the out of plane deformation vibration of C-H groups attached to a *trans* double bond
231 appeared in the spectrum of LDH-ELA as a sharp absorption at 963 cm^{-1} (Fig. 3, Table S3) (Xu
232 et al., 2004).

233 The FT-IR spectrum of LDH-DDS was in accordance with previously reported spectra for
234 dodecylsulfate-intercalated LDH samples (Clearfield et al., 1991). Besides the bands
235 corresponding to the C-H stretching and bending vibrations of the DDS alkyl chains, the
236 spectrum shows the characteristic symmetric and antisymmetric stretching vibration bands of
237 the $-SO_4$ group at 1200 cm^{-1} and 1060 cm^{-1} (Clearfield et al., 1991). The bands at 1377 and
238 1630 cm^{-1} suggest the presence of residual carbonate ions and associated water molecules
239 occupying some of the anion exchange sites. This result was consistent with the chemical
240 analysis of the sample, since in addition to data presented in Table 1, the S content of LDH-
241 DDS (5.0%) indicated a S/Al ratio (S/Al= 0.89) slightly lower than the value expected if all
242 exchange sites in LDH were occupied by DDS anions.
243
244 *3.3. X-ray diffraction analysis: packing of the organic anions in the interlayers*
245 The starting LDH sample prepared in this work exhibited the characteristic XRD pattern of
246 a well crystallized, hydrotalcite-type material, with sharp symmetrical reflections at low angles
247 and low intensity, more asymmetrical reflections at higher angles (Fig. 4) (Donato et al., 2012).
248 The (00l) basal reflections indicated a basal spacing value of 7.7-7.8 Å, in agreement with the
249 presence of carbonate as main interlayer anion (Cavani et al., 1991). The average metal-metal
250 distance was calculated from the (110) diffraction as $2d_{110}$= 3.06 Å, and was also in accordance
251 with the value expected for Mg:Al LDH having a Mg:Al molar ratio of 3:1 (Cavani et al.,
252 1991; Miyata, 1980). The X-ray diffractogram of calcined LDH showed only two broad
253 reflections at 2.09 and 1.48 Å, corresponding to the (200) and (220) diffraction lines of the
254 Mg/Al mixed oxide cubic phase (Barriga et al., 2002; Miyata, 1980; Sato et al., 1986), whereas
255 the diffractogram of the reconstructed LDH sample was almost identical to that of the original
256 LDH, demonstrating that rehydration and carbonation by atmospheric CO_2 led to the successful
257 recovery of the well crystallized, layered structure of the original LDH sample (Costa et al.,
258 2008; Miyata, 1980; Sato et al., 1986).

Intercalation of the organic anions within the galleries of LDH using the reconstruction method led to structures of lower crystallinity compared to both the original and reconstructed LDH samples, as indicated by the reduced X-ray reflection intensities and broadened reflection widths (Fig. 4). Compared to the original LDH, all organo-LDHs showed a shift of the basal reflections to higher *d* values indicating the expansion in the interlamellar distance. The weak reflection at *d*= 7.8 Å could indicate the presence of a small fraction of carbonate-exchanged LDH or be due to higher order (00l) reflection (Costa et al., 2008). The broad halo observed in all samples at about 20º 2ϴ (*d*~ 4.3 Å) can be attributed to the lateral stacking of the organic anion alkyl chains in the LDH interlayer space (Iyi et al., 2009; Kameshima et al., 2006; Zhou et al., 2010).

The basal diffractions of the organo-LDHs are highlighted in the inset in Fig. 4. The basal spacing value obtained for LDH-DDS (25.5 Å) is very similar to the values previously reported by other authors for DDS-exchanged LDH samples (Bruna et al., 2012; Clearfield et al., 1991). Subtracting the layer thickness (4.8 Å) from the basal spacing value (25.5 Å) yields a gallery height of 20.7 Å, which is very similar to the van der Waals end-to-end length of DDS (20.8 Å) (Clearfield et al., 1991). The DDS anions would fit perfectly within this space and could stand perpendicular to the layers with the chains in an all-*trans* conformation (Clearfield et al., 1991).

The basal spacing values for the LDH-fatty acid nanohybrids decreased in the following order: LDH-ELA (40.0 Å) > LDH-OLE (38.5 Å) > LDH-LINO (35.0 Å) > LDH-LINOLEN (32 Å). Clearly, the basal spacing was progressively reduced by the presence of *cis* double bonds in the fatty acid alkyl chain, most likely because the bend imposed by the *cis*-geometry (Fig. 1) led to a reduction in the end-to-end distance of the organic anion, thus reducing the interlayer distance of the resultant LDH-fatty acid nanohybrid.

Figure 5 depicts possible arrangements of ELA, OLE, LINO, and LINOLEN anions in the interlayer space of LDH that are compatible with the measured basal spacing values of the

285 samples. It was assumed that single bonds in the fatty acid alkyl chains were in an all-*trans*
286 conformation and that the chains adopted a tilting angle of about 60º in their interaction with
287 the layers, since this tilting allows both carboxylate oxygen atoms to form hydrogen bonds to
288 the hydroxide layers equally (Meyn et al., 1990; Xu et al., 2004; Zhou et al., 2010). The
289 resulting structures for LDH-ELA and LDH-OLE are very similar to the interdigitated
290 structures proposed by Xu et al. (2004) for 2:1 Zn:Al LDH samples intercalated with oleate
291 and elaidate anions, although the partially interdigitated structure of our (3:1 Mg:Al) LDH-
292 ELA sample (Fig. 5) is in contrast to the almost complete interdigitation proposed by Xu et al.
293 (2004) for their analogous 2:1 Zn/Al sample. The basal spacing of LDH-OLE (38 Å) is,
294 however, essentially identical to the values of 38-39 Å reported by Inomata and Ogawa (2006),
295 Kameshima et al. (2006) and Zhou et al. (2010) for oleate-intercalated Mg/Al LDH samples.
296 Partially interdigitated structures with cointercalated water molecules filling the void spaces
297 between adjacent organic anions were previously proposed by Costantino et al. (1999) for
298 methyl orange intercalation into a hydrotalcite-like compound.
299 For LDH-LINO and LDH-LINOLEN, the structures resulting from assuming single bonds
300 to be in an all-*trans* conformation showed considerable steric hindrance, poor hydrophobic
301 interactions between adjacent alkyl chains, and inefficient compensation of the LDH layer
302 charge (Fig. 5). Such disordered structures appear to be in contradiction with the relatively
303 well-defined basal reflections that were observed in the X-ray diagrams of the samples (Fig. 4).
304 It has previously been pointed out that while saturated fatty acids tend to adopt extended (all
305 *trans*) conformations, unsaturated fatty acids possessing *cis* double bonds separated by
306 methylene carbons exhibit a high degree of flexibility that allows them to adopt folded, as well
307 as extended conformations quite easily (Reggio and Traore, 2000; Small, 1984). This would
308 explain the observation that *cis*-bonds do not prevent relatively dense packing of the chains in
309 lamellar phases (Engelman, 1971; Lagaly et al., 1977). Accordingly, in Figure 6 we propose
310 some of the possible alternative structures resulting from considering that the *cis*-geometry of

311 the double bonds present in OLE, LINO, and LINOLEN promotes the adoption of *gauche*
312 conformations at different points of the alkyl chain for these to achieve nearly-linear
313 conformations. Such conformations would stabilize the structure of the organo-LDHs by
314 improving the hydrophobic interaction between adjacent alkyl chains and by compensating the
315 LDH layer charge more efficiently (Fig. 6).

316 It is interesting to note that each kink imposed by a *cis-gauche* pair would reduce the
317 effective length of the alkyl chain by about 1.25 Å compared to the length exhibited by the
318 same alkyl chain in an all-*trans* conformation (Lagaly et al., 1977), and that this reduction in
319 length represents 1.1 Å of interlayer distance assuming a tilting angle of 60º for the chain. The
320 basal spacing values of our samples (Fig. 4) are close to the values expected assuming that the
321 basal spacing of LDH-ELA (40 Å) is reduced by 2 x 1 kink (2.2 Å) for LDH-OLE (37.8 Å), 2
322 x 2 kinks (4.4 Å) for LDH-LINO (35.6 Å), and 2 x 3 kinks (6.6 Å) for LDH-LINOLEN (33.4
323 Å). The temperature at which the reconstruction reaction was conducted (60º C) should have
324 contributed to overcome the energy barrier (< 3.5 kcal mol^{-1}) for the formation of the *gauche*
325 conformations represented in Figure 6 (Lagaly, 1976).

326 It is also worthy to note that the positions of the FT-IR CH_2 stretching vibration bands at
327 about 2922 and 2852 cm^{-1} have been used as an indication of the *gauche*/*trans* conformer ratio
328 of hydrocarbon chains and, in turn, for monitoring the transition from highly-ordered to more
329 disordered states (Li and Jiang, 2009; Mantsch and McElhaney, 1991). A shift from low
330 wavenumbers, characteristic of highly-ordered, all-*trans* conformations, to higher
331 wavenumbers is usually related to an increase in the number of *gauche* conformers and to the
332 disorder of the chain (Li and Jiang, 2009). The fact that these bands are shifted to higher
333 wavenumbers in LDH-OLE, LDH-LINO, and LDH-LINOLEN compared to their position in
334 LDH-DDS and LDH-ELA (Fig. 3, Table S3) may reflect the disorder of the systems caused by
335 misfits between *gauche*-based conformers of the unsaturated alkyl chains (Fig. 6), which

would also explain the reduced stability of the nanohybrids prepared from *cis*-polyunsaturated fatty acid anions when dispersed in 0.01 M $CaCl_2$.

3.4. Scanning and transmission electron microscopy

Selected samples (LDH, LDH-ELA and LDH-LINOLEN) were examined by scanning (SEM) and transmission (TEM) electron microscopy to get further insight into their morphology and growth habit. SEM analysis confirmed previous observations that inorganic LDH crystallites normally form as platy hexagons with the lateral dimension from 50 nm to a few micrometers, whereas organo-LDH crystallites are frequently sheet-like irregularly shaped and readily bent (Fig. 7) (Xu and Braterman, 2010). Xu and Braterman (2010) proposed that, during the formation of organo-LDHs, adsorption of a layer of organic anion on the metal hydroxide (ab) plane renders a hydrophobic layer which attracts the tails of a second layer of organic anions in an inter-penetrated way. The anionic heads of this second layer of organic anions would be exposed to the aqueous phase and provide the platform for the deposition of a new metal hydroxide sheet. A similar mechanism would be consistent with the inter-digitated structures proposed in Fig. 6 for our samples.

Because LDH crystallites tend to lie flat with the *c* axis perpendicular to the plane of the support, it is in general difficult to directly observe the layer stacking in LDH samples by TEM (Xu et al., 2004). In spite of this, we were able to observe such layer stacking in various regions of LDH-ELA and LDH-LINOLEN (see Figure S1 of the Supplementary information). In such regions, it was not difficult to identify layers separated by distances near 40 Å in LDH-ELA and 32 Å in LDH-LINOLEN, in agreement with the average basal spacing values determined from the XRD analysis of the samples.

3.5. Sorptive properties of the organo-LDHs

The original LDH sample did not sorb any of the tested pesticides (% Sorbed< 5%), whereas the calcined LDH sample displayed some affinity for the acidic pesticides only (% Sorbed= 60-80%). At the pH of the LDH and calcined-LDH dispersions (pH> 7), the neutral pesticides (diuron and alachlor) and the weakly-basic pesticides (atrazine and terbuthylazine, pK_a< 2) existed as uncharged, molecular species and, due to their hydrophobic nature, displayed very little affinity for LDH and calcined-LDH surfaces, which are highly hydrophilic (Celis et al., 2000; Villa et al., 1999; Zhao and Vance, 1998). In contrast, the acidic pesticides (clopyralid and imazethapyr, pK_a< 4) existed as anionic species and significant amounts of these pesticides (60-80%) were sorbed on calcined-LDH by a reconstruction mechanism (Cardoso and Valim, 2006; Celis et al., 1999; Hermosín et al., 1996; Pavlovic et al., 2005; Sato and Okuwaki, 1991; Sato et al., 1986). The lack of sorption of acidic pesticides on the original LDH confirms previous observations that carbonate ions in the interlayers of LDHs display very high affinity for the hydroxide layers and are not replaced by other anions (Celis et al., 1999; Sato et al., 1986).

Incorporation of DDS, ELA, OLE, LINO, and LINOLEN in the interlayers of LDH did not appreciably enhance the affinity of the material for acidic pesticides (clopyralid and imazethapyr) (Table 2). Zeta-potential measurements indicated that, upon modification with the organic anions, the LDH surface changed from positively charged to negatively charged (Figure S2 of the Supplementary information), and electrostatic repulsions probably prevented clopyralid and imazethapyr anions from approaching to the organo-LDH surfaces. In contrast, the performance of the organo-LDHs as sorbents of pesticides existing as uncharged species (diuron, alachlor, atrazine and terbuthylazine) was strongly superior to that of the original and calcined LDH samples (Table 2). The organic phase in the organo-LDHs changed the nature of the sorbent from hydrophilic to hydrophobic, thereby increasing their affinity to the uncharged pesticides by allowing hydrophobic interactions (Celis et al., 2000; Villa et al., 1999; Zhao and Vance, 1998).

Data in Table 2 show that the sorptive properties of the organo-LDHs depended on the nature of the pesticide and also on the organic anion used to prepare the organo-LDH nanohybrid. Under the experimental conditions used, sorption percentages ranged from only 14% for atrazine on LDH-LINOLEN (K_d= 70 L kg^{-1}, K_{oc}= 186 L kg^{-1} C) up to 86% for terbuthylazine on LDH-DDS (K_d= 2370 L kg^{-1}, K_{oc}= 9834 L kg^{-1} C). In general, the performance of every organo-LDH as a pesticide sorbent appeared to increase with the pesticide hydrophobicity or K_{ow} (Table 2). Furthermore, the different organo-LDHs prepared from fatty acid anions, despite having very similar organic carbon contents (Table 1), displayed distinct affinities to a given pesticide; sorption of all pesticides on the organo-LDHs followed the general order: LDH-DDS > LDH-ELA > LDH-OLE > LDH-LINO > LDH-LINOLEN. This sequence appears to indicate that the structures resulting from the incorporation of unsaturated fatty acid anions in the LDH interlayers were less sorptive than those resulting from incorporating saturated organic anions such as DDS, and also that an increasing number of *cis*-unsaturations in the fatty acid alkyl chain further reduces the sorptive capacity of the organo-LDH nanohybrid. Despite that *cis*-unsaturations should have led to less densely packed structures with misfits between the chains, and hence to voids where the pesticide molecules could be hosted, it appears that they also reduced the hydrophobicity of the interlayer organic phase and its performance in the removal of uncharged pesticides.

On the assumption that hydrophobic interactions should have dominated the pesticide sorption process on the organo-LDHs, we plotted the organic carbon-normalized distribution coefficient ($K_{d\text{-}oc}$) for the sorption of each pesticide on the organo-LDHs against the octanol-water partition coefficient of the pesticides (Fig. 8). To directly compare the efficiency of the organic carbon of the organo-LDHs with that of octanol, the pesticide K_{ow} values were also normalized to the organic carbon content of octanol (0.608 kg L^{-1}) (Fig. 8). The linear relationships observed in Fig. 8 strongly support that pesticide sorption on the organo-LDHs was a function of the pesticide hydrophobicity or K_{ow} value, and further show that such a $K_{d\text{-}oc}$-

413 K_{ow} relationship varies depending on the structural characteristics of the sorbent, and
414 specifically, on the degree and type of unsaturation in the organic anion alkyl chain. The slopes
415 > 1 observed for LDH-DDS and LDH-ELA indicate that the organic C of these organo-LDHs
416 had greater affinity to the pesticides than that of octanol, whereas the slopes < 1 observed for
417 LDH-OLE, LDH-LINO, and LDH-LINOLEN indicate that the organic C of these organo-
418 LDHs had less affinity to the pesticides than that of octanol.
419
420 **4. Conclusions**
421 Intercalation of several long-chain (C18) unsaturated fatty acid anions into Mg/Al (3:1)
422 LDH showed that the degree and type of unsaturation in the fatty acid alkyl chain are important
423 factors determining the structure and sorptive properties of LDH-fatty acid nanohybrid
424 materials. In particular, the bend imposed by the *cis* geometry of the double bonds present in
425 fatty acid anions such as oleate, linoleate, and linolenate, resulted in less densely packed (less
426 stable) structures and reduced the interlayer distance of the resultant organo-LDH nanohybrid
427 compared to the structure resulting from intercalation of the analogous linear *trans*-unsaturated
428 elaidate anion. *Cis*-unsaturated fatty acid anions also yielded organo-LDHs with less affinity to
429 uncharged pesticides than organo-LDHs prepared from incorporation of dodecylsulfate and
430 *trans*-unsaturated fatty acid anions, presumably because they led to structures with reduced
431 hydrophobicity. Two important environmental implications can be derived from these results.
432 First, they demonstrate that subtle differences in the structural properties of the organic anion
433 used as a modifier of LDHs can strongly affect the performance of the resultant nanohybrid as
434 a sorbent of organic pollutants. Second, they are a direct evidence of the increasing realization
435 that not only the amount, but also the chemical characteristics of organic matter, can influence
436 the sorption properties of organomineral soil colloids (Ahangar et al., 2008; Celis et al., 2006;
437 Karapanagioti et al., 2000), questioning the validity of universal K_{oc}-K_{ow} relationships

commonly used to predict the sorption of hydrophobic organic compounds in soils (Renner, 2002).

Acknowledgments

This work has been financed by the Spanish Ministry of Economy and Competitiveness (MINECO Project AGL2011-23779) and Junta de Andalucía (JA Projects P07-AGR-03077 and P11-AGR-7400 and Research Group AGR-264), cofinanced with European FEDER-FSE funds (Operative Program 2007-2013). B. Gámiz thanks JA for a post-doctoral contract linked to the project P07-AGR-03077. M.A. Adelino thanks MINECO for her pre-doctoral FPI fellowship. The authors thank Dr. F. Bruna for his help in the sample preparation.

Supplementary information

Table S1. Some characteristics of the pesticides used in sorption experiments. Table S2. Chromatographic conditions used for the analysis of the pesticides by HPLC. Table S3. Proposed assignments for FT-IR bands of organo-LDH samples. Fig. S1. TEM micrographs of LDH-ELA and LDH-LINOLEN samples. Fig. S2. Z-potential distribution curves for LDH and organo-LDH samples.

References

Ahangar, A.G., Smernik, R.J., Kookana, R.S., Chittleborough, D.J., 2008. Clear effects of soil organic matter chemistry, as determined by NMR spectroscopy, on the sorption of diuron. *Chemosphere* 70, 1153-1160.

Ayala-Luis, K.B., Koch, C.B., Hansen, H.C.B., 2010. Intercalation of linear C9-C16 carboxylates in layered Fe^{II}-Fe^{III}-hydroxides (green rust) via ion exchange. *Applied Clay Science* 48, 334-341.

Barriga, C., Gaitán, M., Pavlovic, I., Ulibarri, M.A., Hermosín, M.C., Cornejo, J., 2002. Hydrotalcites as sorbent for 2,4,6-trinitrophenol: influence of the layer composition and interlayer anion. *Journal of Materials Chemistry* 12, 1027-1034.

Borja, M., Dutta, P.K., 1992. Fatty acids in layered metal hydroxides: membrane-like structure and dynamics. The *Journal of Physical Chemistry* 96, 5434-5444.

Bruna, F., Celis, R., Real, M., Cornejo, J., 2012. Organo/LDH nanocomposite as an adsorbent of polycyclic aromatic hydrocarbons in water and soil-water systems. *Journal of Hazardous Materials* 225-226, 74-80.

Cardoso, L.P., Valim, J.B., 2006. Study of acids herbicides removal by calcined Mg-Al-CO_3-LDH. *Journal of Physics and Chemistry of Solids* 67, 987-993.

Carlino, S., 1997. The intercalation of carboxylic acids into layered double hydroxides: a critical evaluation and review of the different methods. *Solid State Ionics* 98, 73-84.

Cavani, F., Tirifò, F., Vaccari, A., 1991. Hydrotalcite-type anionic clays: preparation, properties and applications. *Catalysis Today* 11, 173-301.

Celis, R., de Jonge, H., de Jonge, L.W., Real, M., Hermosín, M.C., Cornejo, J., 2006. The role of mineral and organic components in phenanthrene and dibenzofuran sorption by soil. *European Journal of Soil Science* 57, 308-319.

Celis, R., Koskinen, W.C., Cecchi, A.M., Bresnahan, G.A., Carrizosa, M.J., Ulibarri, M.A., Pavlovic, I., Hermosin, M.C., 1999. Sorption of the ionizable pesticide imazamox by organo-clays and organohydrotalcites. *Journal of Environmental Science and Health Part B* 34, 929-941.

Celis, R., Koskinen, W.C., Hermosín, M.C., Ulibarri, M.A., Cornejo, J., 2000. Triadimefon interactions with organoclays and organohydrotalcites. *Soil Science Society of America Journal* 64, 36-43.

Chibwe, K., Jones, W., 1989. Intercalation of organic and inorganic anions into layered double hydroxides. *Journal of the Chemical Society-Chemical Communications* 14, 926-927.

489 Clearfield, A., Kieke, M., Kwan, J., Colon, J.L., Wang, R.C., 1991. Intercalation of dodecyl
490 sulfate into layered double hydroxides. *Journal of Inclusion Phenomena and Molecular*
491 *Recognition in Chemistry* 11, 361-378.
492 Cornejo, J., Celis, R., Pavlovic, I., Ulibarri, M.A., 2008. Interactions of pesticides with clays
493 and layered double hydroxides: a review. *Clay Minerals* 43, 155-175.
494 Costa, F.R., Leuteritz, A., Wagenknecht, U., Jehnichen, D., Häußler, L., Heinrich, G., 2008.
495 Intercalation of Mg-Al layered double hydroxide by anionic surfactants: preparation and
496 characterization. *Applied Clay Science* 38, 153-164.
497 Costantino, U., Coletti, N., Nocchetti, M., Aloisi, G.G., Elisei, F., 1999. Anion exchange of
498 methyl orange into Zn-Al synthetic hydrotalcite and photophysical characterization of the
499 intercalates obtained. *Langmuir* 15, 4454-4460.
500 Costantino, U., Gallipoli, A., Nocchetti, M., Camino, G., Bellucci, F., Frache, A., 2005. New
501 nanocomposites constituted of polyethylene and organically modified ZnAl-hydrotalcites.
502 *Polymer Degradation and Stability* 90, 586-590.
503 Costantino, U., Nocchetti, M., Sisani, M., Vivani, R., 2009. Recent progress in the synthesis
504 and application of organically modified hydrotalcites. *Zeitschrift für Kristallographie* 224,
505 273-281.
506 Cruz-Guzmán, M., Celis, R., Hermosín, M.C., Cornejo, J., 2004. Adsorption of the herbicide
507 simazine by montmorillonite modified with natural organic cations. *Environmental Science*
508 *& Technology* 38, 180-186.
509 Del Arco, M., Martín, C., Martín, I., Rives, V., Trujillano, R., 1993. A FTIR spectroscopic
510 study of surface acidity and basicity of mixed Mg, Al-oxides obtained by thermal
511 decomposition of hydrotalcite. *Spectrochimica Acta Part A* 49, 1575-1582.
512 Donato, R.K., Luza, L., da Silva, R.F., Moro, C.C., Guzatto, R., Samios, D., Mateja, L.,
513 Dimzoski, B., Amico, S.C., Schrekker, H.S., 2012. The role of oleate-functionalized layered

514 double hydroxide in the melt compounding of polypropylene nanocomposites. *Materials*
515 *Science and Engineering C* 32, 2396-2403.
516 Engelman, D.M., 1971. Lipid bilayer structure in the membrane of *Mycoplasma laidlawii*.
517 *Journal of Molecular Biology* 58, 153-165.
518 Goh, K.H., Lim, T.T., Dong, Z., 2009. Enhanced arsenic removal by hydrothermally treated
519 nanocrystalline Mg/Al layered double hydroxide with nitrate intercalation. *Environmental*
520 *Science & Technology* 43, 2537-2543.
521 Hermosín, M.C., Pavlovic, I., Ulibarri, M.A., Cornejo, J., 1993. Trichlorophenol adsorption on
522 layered double hydroxide: a potential sorbent. *Journal of Environmental Science and Health*
523 *Part A* 28, 1875-1888.
524 Hermosín, M.C., Pavlovic, I., Ulibarri, M.A., Cornejo, J., 1996. Hydrotalcite as sorbent for
525 trinitrophenol: sorption capacity and mechanism. *Water Research* 30, 171-177.
526 Hernández-Moreno, M.J., Ulibarri, M.A., Rendón, J.L., Serna, C.J., 1985. IR characteristics of
527 hydrotalcite-like compounds. *Physics and Chemistry of Minerals* 12, 34-38.
528 Inacio, J., Taviot-Guého, C., Forano, C., Besse J.P., 2001. Adsorption of MCPA pesticide by
529 MgAl-layered double hydroxides. *Applied Clay Science* 18, 255-264.
530 Inomata, K., Ogawa, M., 2006. Preparation and properties of Mg/Al layered double hydroxide-
531 oleate and -stearate intercalation compounds. *Bulletin of the Chemical Society of Japan* 79,
532 336-342.
533 Iyi, N., Tamura, K., Yamada, H., 2009. One-pot synthesis of organophilic layered double
534 hydroxides (LDHs) containing aliphatic carboxylates: extended “homogeneous
535 precipitation” method. *Journal of Colloid and Interface Science* 340, 67-73.
536 Kameshima, Y., Yoshizaki, H., Nakajima, A., Okada, K., 2006. Preparation of sodium
537 oleate/layered double hydroxide composites with acid-resistant properties. *Journal of*
538 *Colloid and Interface Science* 298, 624-628.

539 Kanicky, J.R., Shah, D., 2002. Effect of degree, type, and position of unsaturation on the pK_a
540 of long-chain fatty acids. *Journal of Colloid and Interface Science* 256, 201-207.
541 Karapanagioti, H.K., Kleineidam, S., Sabatini, D.A., Grathwohl, P., Ligouis, B, 2000. Impacts
542 of heterogeneous organic matter on phenanthrene sorption: equilibrium and kinetic studies
543 with aquifer material. *Environmental Science & Technology* 34, 406-414.
544 Kuehn, T., Pollmann, H., 2010. Synthesis and characterization of Zn-Al layered double
545 hydroxides intercalated with 1- to 19-carbon carboxylic acid anions. *Clays and Clay*
546 *Minerals* 58, 596-605.
547 Lagaly, G., 1976. Kink-block and gauche-block structures of biomolecular films. *Angewandte*
548 *Chemie International Edition* 15, 575-586.
549 Lagaly, G., 2001. Pesticide-clay interactions and formulations. *Applied Clay Science* 18, 205-
550 209.
551 Lagaly, G., Weiss, A., Stuke, E., 1977. Effect of double-bonds on biomolecular films in
552 membrane models. *Biochimica et Biophysica Acta* 470, 331-341.
553 Li, Z., Jiang, W.T., 2009. Interlayer conformations of intercalated dodecyltrimethylammonium
554 in rectorite as determined by FTIR, XRD, and TG analyses. *Clays and Clay Minerals* 57,
555 194-204.
556 Mantsch, H.H., McElhaney, R.N., 1991. Phospholipid phase transitions in model and
557 biological membranes as studied by infrared spectroscopy. *Chemistry and Physics of Lipids*
558 57, 213-226.
559 Meyn, M., Beneke, K., Lagaly, G., 1990. Anion-exchange reactions of layered double
560 hydroxides. *Inorganic Chemistry* 29, 5201-5207.
561 Miyata, S., 1980. Physicochemical properties of synthetic hydrotalcites in relation to
562 composition. *Clays and Clay Minerals* 28, 50-56.
563 Miyata, S., Kumura, T., 1973. Synthesis of new hydrotalcite-like compounds and their
564 physico-chemical properties. *Chemistry Letters* 2, 843-848.

565 Narita, E., Kaviratna, P., Pinnavaia, T.J., 1991. Synthesis of heteropolyoxometalate pillared
566 double hydroxides via calcined zinc-aluminum oxide precursors. *Chemistry Letters* 5, 805-
567 808.
568 Newman, S.P., Jones, W., 1998. Synthesis, characterization and applications of layered double
569 hydroxides containing organic guests. *New Journal of Chemistry* 22, 105-115.
570 Paek, S.M., Oh, J.M., Choy, J.H., 2011. A lattice-engineering route to heterostructured
571 functional nanohybrids. *Chemistry Asian Journal* 6, 324-338.
572 Pavlovic, I., Barriga, C., Hermosín, M.C., Cornejo, J., Ulibarri, M.A., 2005. Adsorption of
573 acidic pesticides 2,4-D, Clopyralid and Picloram on calcined hydrotalcite. *Applied Clay*
574 *Science* 30, 125-133.
575 Pavlovic, I., Ulibarri, M.A., Hermosín, M.C., Cornejo, J., 1997. Sorption of an anionic
576 surfactant from water by a calcined hydrotalcite-like sorbent. *Fresenius Environmental*
577 *Bulletin* 6, 266-271.
578 Reggio, P.H., Traore, H., 2000. Conformational requirements for endocannabinoid interaction
579 with the cannabinoid receptors, the anandamide transporter and fatty acid amidohydrolase.
580 *Chemistry and Physics of Lipids* 108, 15-35.
581 Reichle, W.T., 1986. Synthesis of anionic clay minerals (mixed metal hydroxides,
582 hydrotalcite). *Solid State Ionics* 22, 135-141.
583 Renner, R., 2002. The K_{ow} controversy. *Environmental Science & Technology* 36, 411A-413A.
584 Rives, V. (Ed.), 2001. Layered Double Hydroxides: Present and Future. Nova Science
585 Publishers, Inc. New York.
586 Sato, T., Okuwaki, A., 1991. Intercalation of benzenecarboxylate ions into the interlayer of
587 hydrotalcite. *Solid State Ionics* 45, 43-48.
588 Sato, T., Wakabayashi, T., Shimada, M., 1986. Adsorption of various anions by magnesium
589 aluminum oxide ($Mg_{0.7}Al_{0.3}O_{1.15}$). *Industrial and Engineering Chemistry Product Research*
590 *and Development* 25, 89-92.

591 Small, D.M., 1984. Lateral chain packing in lipids and membranes. *Journal of Lipid Research*,
592 *25*, 1490-1500.
593 Villa, M.V., Sánchez-Martín, M.J., Sánchez-Camazano, M., 1999. Hydrotalcites and organo-
594 hydrotalcites as sorbents for removing pesticides from water. *Journal of Environmental*
595 *Science and Health Part B* 34, 509-525.
596 Xu, Z.P., Braterman, P.S., 2010. Synthesis, structure and morphology of organic layered
597 double hydroxide (LDH) hybrids: comparison between aliphatic anions and their
598 oxygenated analogs. *Applied Clay Science* 48, 235-242.
599 Xu, Z.P., Braterman, P.S., Yu, K., Xu, H., Wang, Y., Brinker, C.J., 2004. Unusual hydrocarbon
600 chain packing mode and modification of crystalline growth habit in the self-assembled
601 nanocomposites zinc-aluminum –hydroxide oleate and elaidate (*cis*- and *trans*-
602 $[Zn_2Al(OH)_6(CH_3(CH_2)_7CH=CH(CH_2)_7COO^-)]$ and magnesium analogues. *Chemistry of*
603 *Materials* 16, 2750-2756.
604 Zhao, H., Nagy, K.L., 2004. Dodecyl sulfate-hydrotalcite nanocomposites for trapping
605 chlorinated organic pollutants in water. *Journal of Colloid and Interface Science* 274, 613-
606 624.
607 Zhao, H., Vance, G.F., 1998. Molecular inclusion properties of hydrophobic organic
608 compounds by a modified β-cyclodextrin intercalated within a layered double hydroxide.
609 *Journal of Inclusion Phenomena and Molecular Recognition in Chemistry* 31, 305-317.
610 Zhou, Q., Verney, V., Commereuc, S., Chin, I.J., Leroux, F., 2010. Strong interfacial attrition
611 developed by oleate/layered double hydroxide nanoplatelets dispersed into poly(butylene
612 succinate). *Journal of Colloid and Interface Scienc*e 349, 127-133.

FIGURE CAPTIONS

Fig. 1. Chemical structures of the organic anions used to prepare the organo-LDHs.

Fig. 2. Chemical structures of the pesticides.

Fig. 3. FT-IR spectra of LDH, calcined LDH, reconstructed LDH, and organo-LDH samples.

Fig. 4. Powder X-ray diffractograms of LDH, calcined LDH, reconstructed LDH, and organo-LDH samples.

Fig. 5. Proposed structures for LDH-ELA, LDH-OLE, LDH-LINO, and LDH-LINOLEN, with all single bonds of the fatty acid anions in a *trans* conformation. The scale bar corresponds to a distance of about 6 Å.

Fig. 6. Possible structures for LDH-OLE, LDH-LINO, and LDH-LINOLEN where the fatty acid anions contain one (OLE), two (LINO) or three (LINOLEN) single bonds in *gauche* conformation to achieve a pseudo-linear arrangement of the alkyl chains. The scale bar corresponds to a distance of about 6 Å.

Fig. 7. SEM micrographs of LDH, LDH-ELA and LDH-LINOLEN samples.

Fig. 8. Relationships between the experimental $K_{d\text{-}oc}$ values obtained for the sorption of several pesticides on the organo-LDHs and the pesticide octanol-water partition coefficients (K_{ow}) normalized to the organic carbon content of octanol: K_{oc} (octanol)= K_{ow}/0.608.

Table 1

Chemical composition of the samples prepared and proposed formulae.

Sample	Mass (%)			Molar ratios			Proposed formula
	Mg	Al	C	x	Mg/Al	C/Al	
LDH	23.3	8.2	2.2	0.24	3.1	0.60	$Mg_{3.04}Al_{0.96}(OH)_8(CO_3)_{0.58}\cdot 2.6H_2O$
Calcined LDH	40.2	13.9	0.8	0.24	3.2	0.13	$Mg_{6.11}Al_{1.93}O_9\cdot 1.5H_2O$
LDH-ELA	12.8	4.5	39.0	0.24	3.2	19.5	$Mg_{3.04}Al_{0.96}(OH)_8(ELA)_{1.04}\cdot 2.5H_2O$
LDH-OLE	12.2	4.4	38.4	0.24	3.1	19.9	$Mg_{3.04}Al_{0.96}(OH)_8(OLE)_{1.06}\cdot 3.5H_2O$
LDH-LINO	12.4	4.3	38.0	0.24	3.2	19.9	$Mg_{3.04}Al_{0.96}(OH)_8(LINOLE)_{1.06}\cdot 3.8H_2O$
LDH-LINOLEN	12.0	4.1	37.6	0.24	3.2	20.4	$Mg_{3.04}Al_{0.96}(OH)_8(LINOLEN)_{1.08}\cdot 4.6H_2O$
LDH-DDS	13.7	4.8	24.1	0.24	3.2	11.3	$Mg_{3.04}Al_{0.96}(OH)_8(DDS)_{0.91}\cdot 3.6H_2O$

Table 2

Sorption percentages, Sorbed (%), and distribution coefficients, K_d (L kg^{-1}), for different pesticides on the organo-LDHs[a].

Pesticide name	Pesticide K_{ow} (P)	LDH-DDS		LDH-ELA		LDH-OLE		LDH-LINO		LDH-LINOLEN	
		Sorbed (%)	K_d (L kg^{-1})	Sorbed (%)	K_d (L kg^{-1})	Sorbed (%)	K_d (L kg^{-1})	Sorbed (%)	K_d (L kg^{-1})	Sorbed (%)	K_d (L kg^{-1})
Clopyralid	0.002	< 5	-	< 5	-	< 5	-	< 5	-	< 5	-
Imazethapyr	30	6	20	10	40	< 5	-	< 5	-	< 5	-
Atrazine	500	40	270	36	230	32	140	18	90	14	70
Diuron	740	61	630	28	156	28	156	15	70	30	170
Alachlor	1230	76	1250	75	1180	71	980	49	380	33	200
Terbuthylazine	2510	86	2370	83	1950	74	1140	71	980	50	400

[a] Sorbed: percentage of pesticide sorbed from a 1 mg L^{-1} initial pesticide aqueous solution (20 mg : 8 mL sorbent : solution ratio).

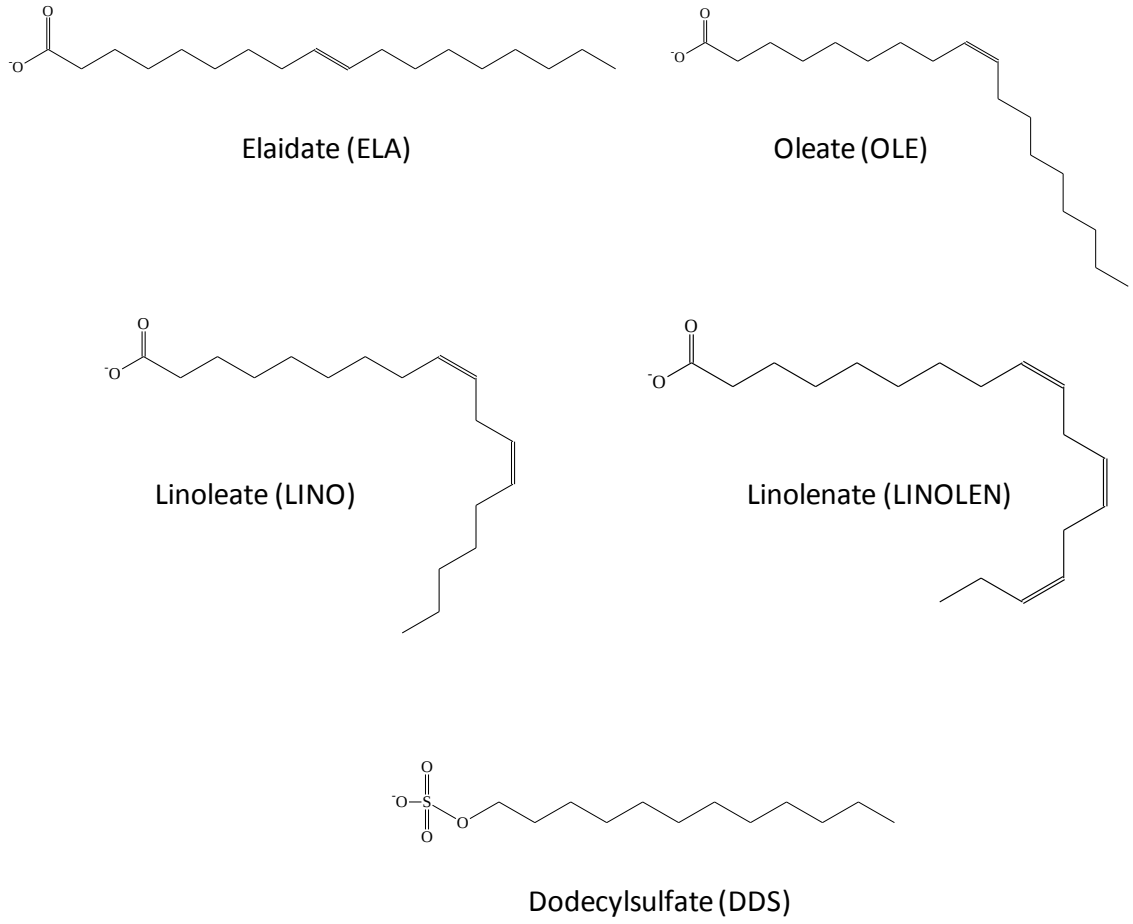

Fig. 1. Chemical structures of the organic anions used to prepare the organo-LDHs.

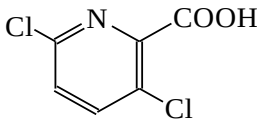

Clopyralid

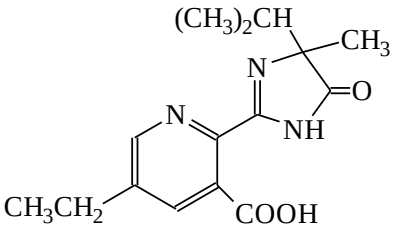

Imazethapyr

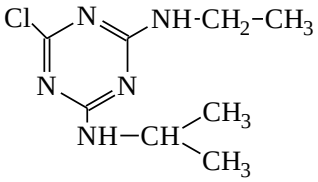

Atrazine

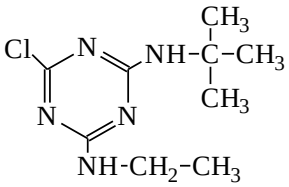

Terbuthylazine

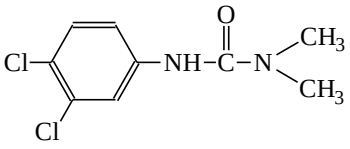

Diuron

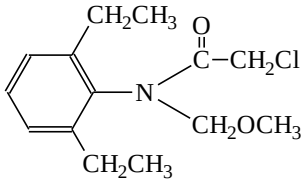

Alachlor

Fig. 2. Chemical structures of the pesticides.

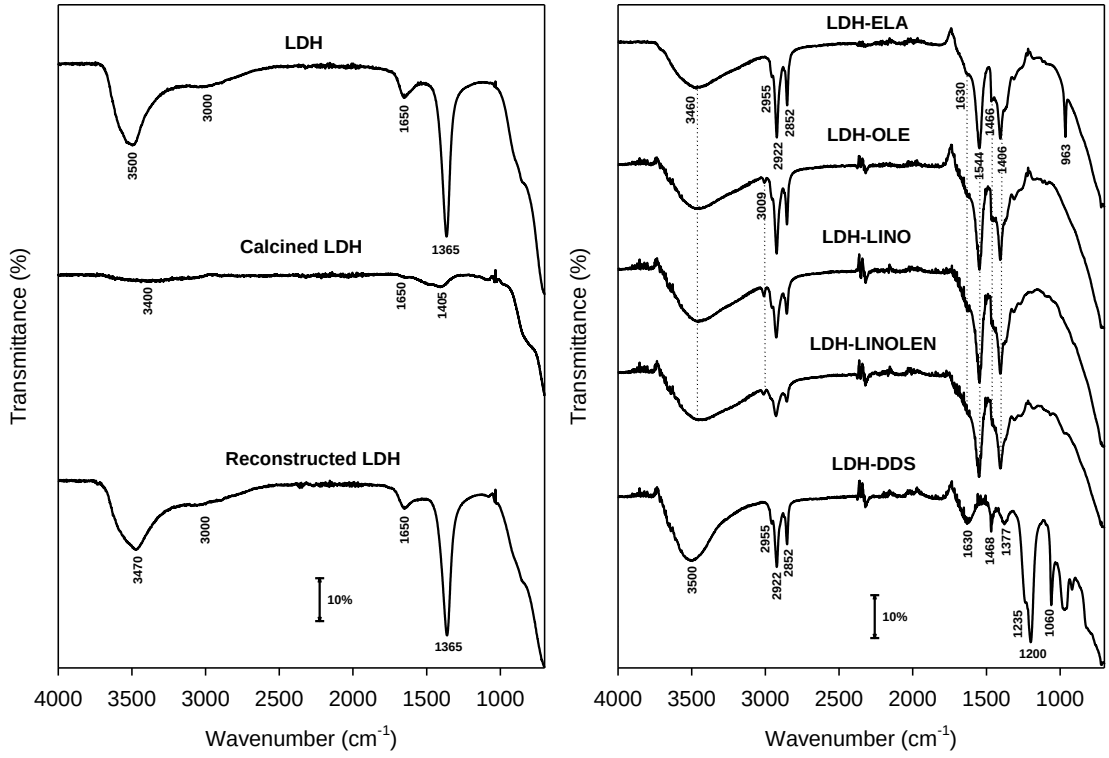

Fig. 3. FT-IR spectra of LDH, calcined LDH, reconstructed LDH, and organo-LDH samples.

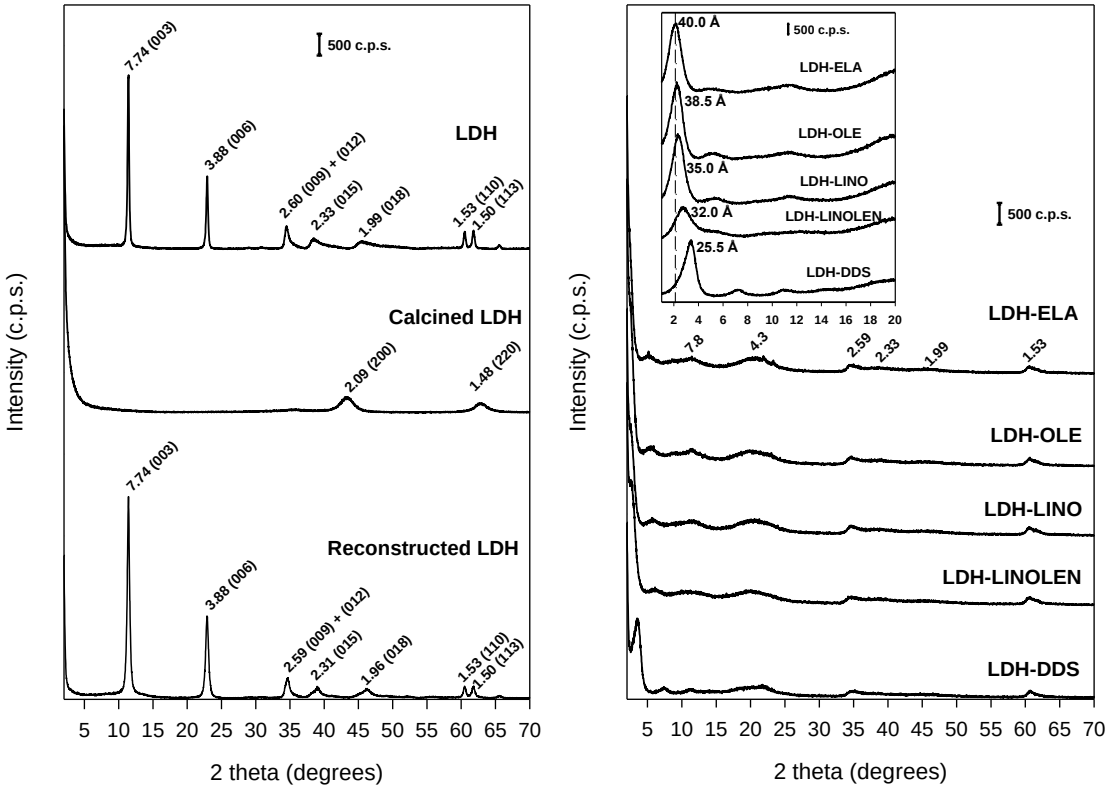

Fig. 4. Powder X-ray diffractograms of LDH, calcined LDH, reconstructed LDH, and organo-LDH samples.

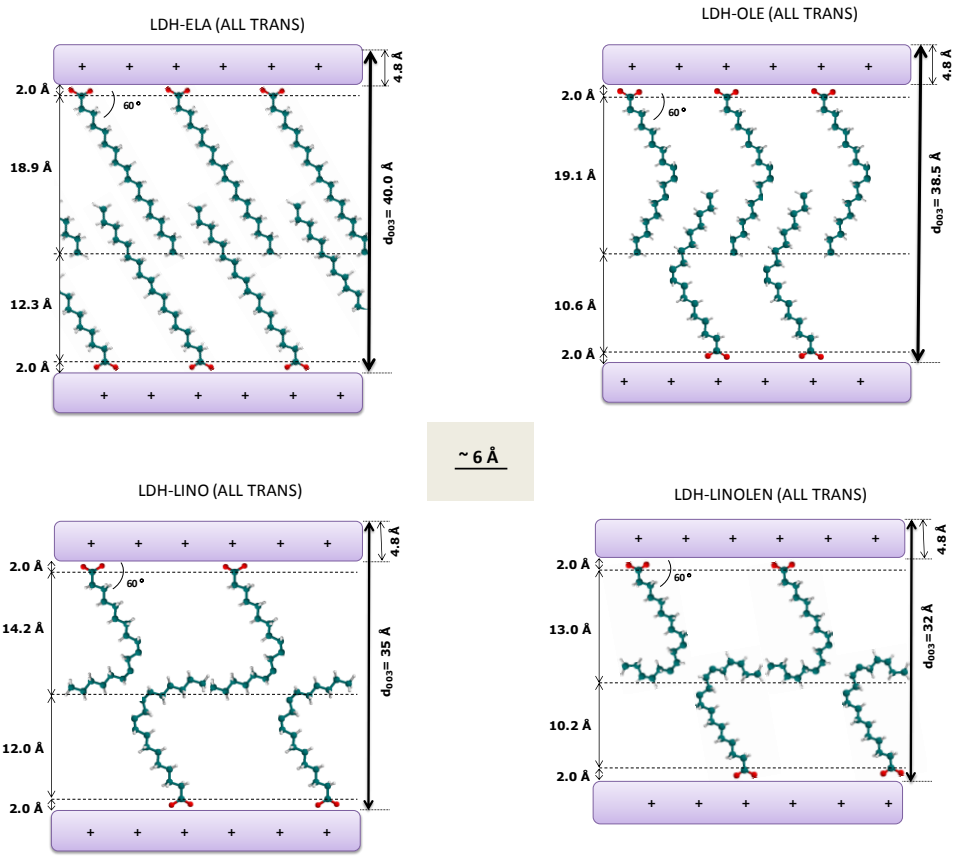

Fig. 5. Proposed structures for LDH-ELA, LDH-OLE, LDH-LINO, and LDH-LINOLEN, with all single bonds of the fatty acid anions in a *trans* conformation. The scale bar corresponds to a distance of about 6 Å.

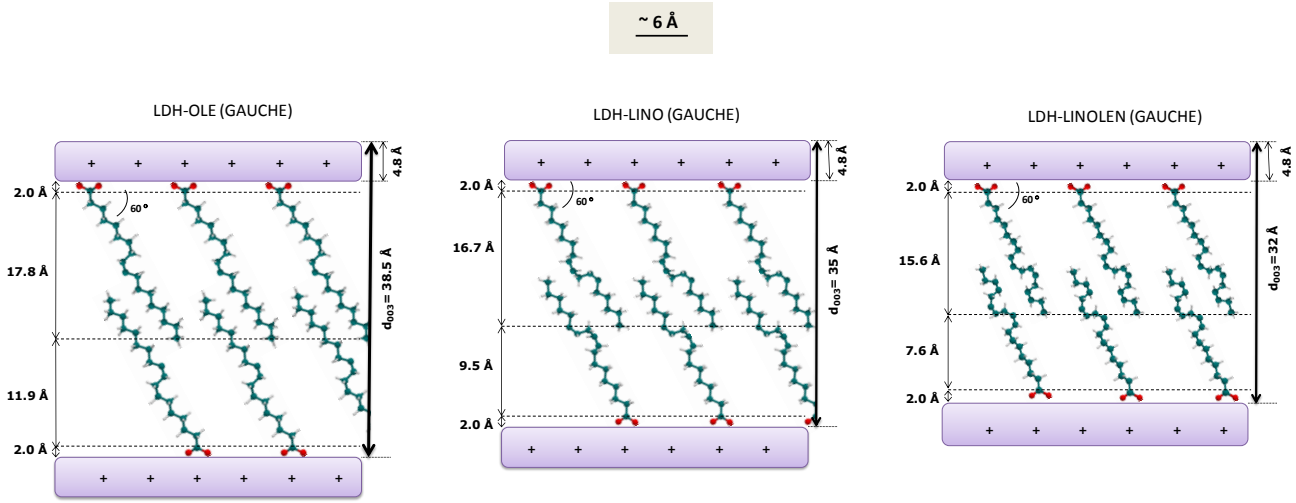

Fig. 6. Possible structures for LDH-OLE, LDH-LINO, and LDH-LINOLEN where the fatty acid anions contain one (OLE), two (LINO) or three (LINOLEN) single bonds in *gauche* conformation to achieve a pseudo-linear arrangement of the alkyl chains. The scale bar corresponds to a distance of about 6 Å.

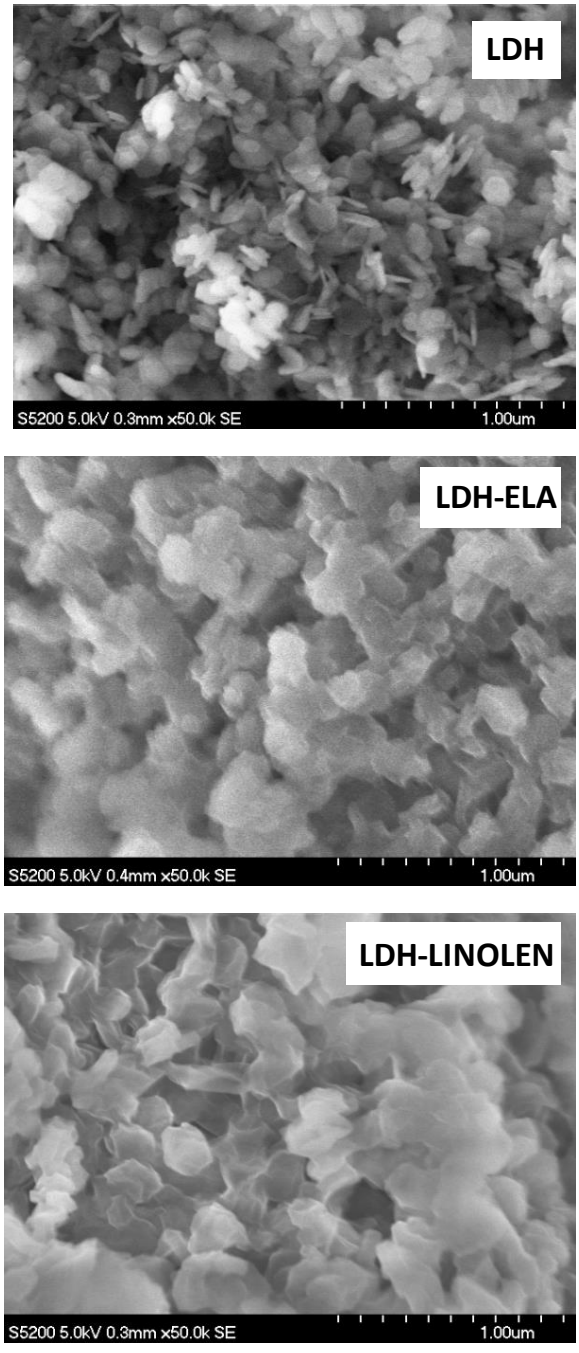

Fig. 7. SEM micrographs of LDH, LDH-ELA and LDH-LINOLEN samples.

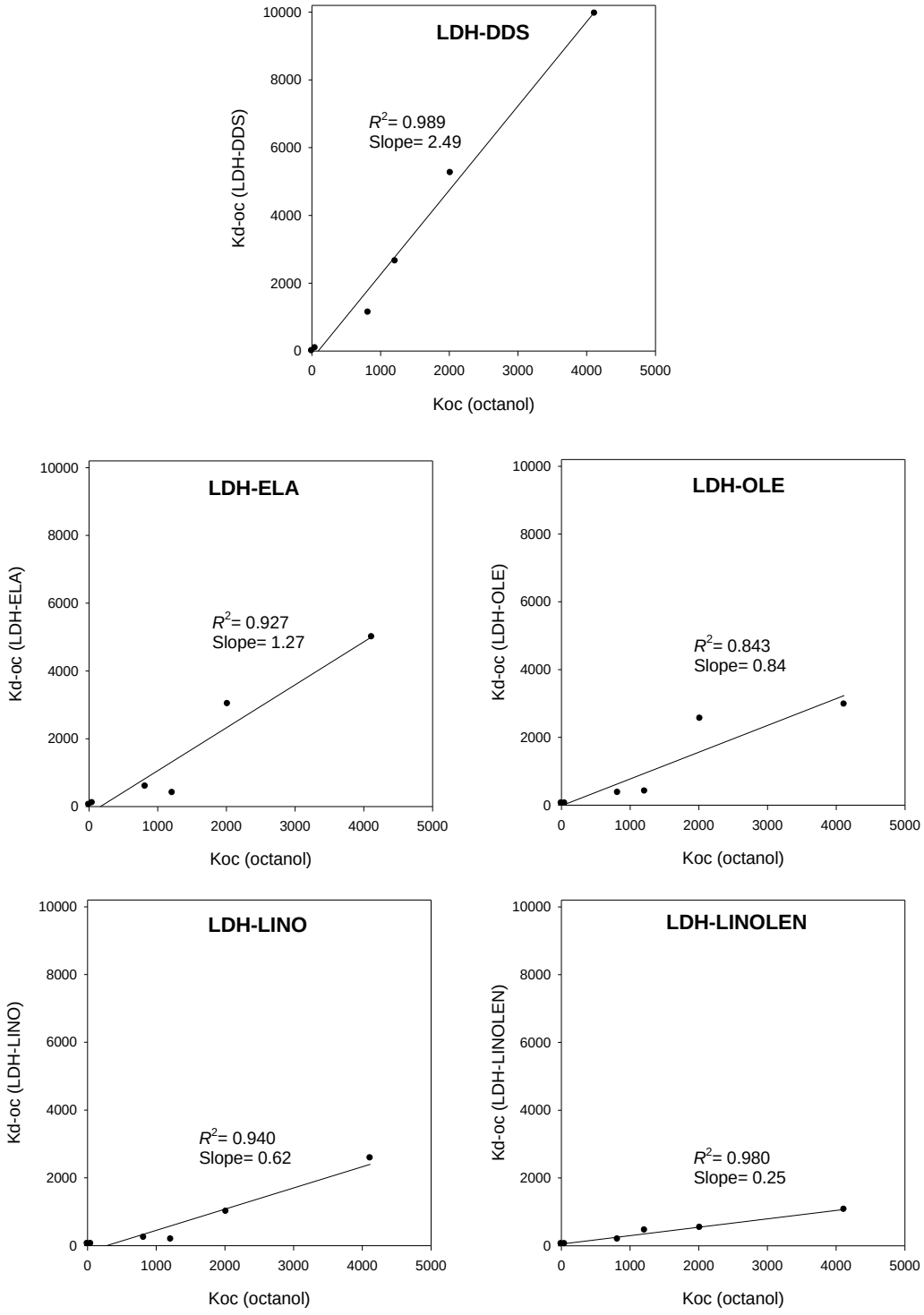

Fig. 8. Relationships between the experimental $K_{d\text{-}oc}$ values obtained for the sorption of several pesticides on the organo-LDHs and the pesticide octanol-water partition coefficients (K_{ow}) normalized to the organic carbon content of octanol: K_{oc} (octanol)= K_{ow}/0.608.